Colloidal and Thermal Characteristics of Concentrated Dispersions of Polymethacrylate-Based Latices for Aqueous Enteric Coating

MATTIAS PAULSSON[†] AND SATISH K. SINGH[*,‡,§]

Contribution from *Department of Pharmacy, Division of Pharmaceutics, Uppsala University, Uppsala Biomedical Centre, Box 580, S-751 23 Uppsala, Sweden, and Department of Pharmaceutical Technology, Pharmacia & Upjohn AB, S-751 82 Uppsala, Sweden.*

Received August 31, 1998. Accepted for publication December 10, 1998.

Abstract □ We have used rheological and thermal methods to study the colloidal characteristics of a widely used technical latex. The dispersions of poly(methacrylic acid–ethyl acrylate) (Eudragit L100-55) were found to be stabilized by a combination of electrostatic and steric mechanisms termed as electrosteric stabilization. The electrosteric stabilization is considered to arise in part from dissolved polymer chains with charged carboxylic groups extending out into the continuous phase. The presence of dissolved polymer chains in the dispersion implies that coalescence and interpenetration will be facilitated during film formation, enabling a smooth continuous film to be formed. The extent of the stabilization layer and an effective hard-sphere volume was estimated to discuss the steady shear and viscoelastic properties in this context. The glass transition temperature (T_g) of the particles making up the dispersion has also been determined as a function of sorbed moisture and modeled by the Gordon–Taylor equation modified for specific interaction between water, surfactant, and polymer. This parameter at high moisture content can be used as a first approximation to the minimum film-forming temperature (MFT). Change in T_g (and thus MFT) with moisture content implies that the coating process must be controlled so as to produce a rate of drying slow enough to allow coalescence to occur.

Introduction

The release of drug from a solid dosage form is often tailored by applying a polymeric coating. Water-based rate-controlling polymer films are generally made by spraying an aqueous polymeric dispersion (latex) onto the dosage form (tablet or multiparticulates) and then evaporating the water, a process not unlike film formation from water-borne paints. Commonly used aqueous coating polymers within the pharmaceutical industry are cellulose derivatives and acrylic polymers. These latices are characterized by low viscosity, even at relatively high solid content.[1]

The mechanism of film formation from aqueous latex dispersions has been discussed for almost half a century. The evolution of the theories of film formation can be followed through a number of interesting papers.[2−5] Rheology,[4,6] scanning electron microscopy,[4,6] and lately atomic force microscopy[4,7] are primary techniques that have been employed for studying dispersions and film formation. Latex dispersions are subject to a range of shear rates during the coating process ranging from 10^5 s^{-1} during atomization to 10^{-2} s^{-1} during leveling. The process of deformation and coalescence is a function of polymer viscoelasticity.[2] In this work, we have applied rheology to study a commercial latex dispersion based on a methacrylic acid−ethyl acrylate (MAEA) copolymer and relate its characteristics to the first stages of film formation in pharmaceutical processing.

Film formation from polymer dispersions is correlated to the glass transition temperature (T_g) of the polymer and the temperature of operation in relation to the minimum film-forming temperature (MFT) of the latex.[8] The MFT is the minimum temperature above which a continuous and clear film is formed during drying.[2,8] While film formation does not imply that interdiffusion of polymer chains between adjacent particles must occur,[7,9] coalescence and interpenetration would be required for the formation of a strong film.[5] This flexibility is influenced by additives (plasticizers) as well as water (moisture) content of the polymer and can be detected as a reduction in both the T_g and the MFT. While both these parameters are apparently similar, T_g is a fundamental property of the material while MFT is an ill-defined parameter[10] reflecting latex morphology[11] and even particle size in some cases[2]. T_g can, however, be used as a first approximation for the MFT. (Data from Heuts et al.[8] gives the ratio of MFT to T_g as ranging between 0.8 and 1.1 for single stage acrylic dispersions, while data from Hoy[12] gives a ratio of 0.95). The T_g (and MFT) of the sprayed latex will change with moisture content, and a poor film will be formed if the MFT rises above operating temperature due to too rapid a drying. We have therefore determined the moisture adsorption isotherm for the dry commercial latex dispersion and measured the T_g of as a function of moisture content.

Materials and Methods

A spray-dried aqueous dispersion of methacrylic acid−ethyl acrylate (MAEA) copolymer (MW 250 000) with the commercial name Eudragit L100-55 was used (Röhm GmbH, Darmstadt, Germany). The as-received Eudragit L100-55 also contains 0.7% sodium lauryl sulfate (SLS) and 2.3% Polysorbate 80 based on solid substance, added to function as emulsifiers.

Dispersions were made by adding NaOH to the latex particle agglomerates in water and dispersing in accordance with Lehmann.[1] The dispersion is stable when 3−6% of the carboxylic groups of the copolymer are ionized; at greater than 20% ionization, the polymer particles would dissolve.[1] A suitable ratio of alkali and polymer was found to be 90 g of polymer/g of NaOH. This ratio was determined by measuring the viscosity and stability of the dispersions with constant polymer content but varying alkali concentration. Low pH gave an unstable dispersion while high pH's resulted in a rapid increase in viscosity due to dissolution of polymer. Dispersions were considered to be stable if no sedimentation could be detected in 24 h by visual inspection. The pH of the dispersions ranged between 5.1 and 5.3 (see Table 1). By keeping the NaOH−MAEA ratio constant, stable dispersions over a wide

* Corresponding author.
† Uppsala University.
‡ Pharmacia & Upjohn AB.
§ Present address: Pharmacia & Upjohn, Inc. 7207-259-277, 7000 Portage Rd., Kalamazoo, MI 49001-0199. Fax: +1-616-833-6743. E-mail: satish.singh@am.pnu.com.

10.1021/js9803555 CCC: $18.00
Published on Web 03/13/1999

Table 1—Estimation of the Effective Hydrodynamic Volume Fraction. The Increase of Effective Particle Radius (Δ) is Obtained from a Krieger–Dougherty Data Fit ($n = 3$)

ϕ	ϕ_{eff}	η_r	Δ (nm)	pH
0.255 ± 0.0003	0.456618	54.4	21.43325	5.27 ± 0.05
0.292 ± 0.004	0.493944	124	19.15116	5.20 ± 0.02
0.335 ± 0.005	0.492656	120	13.71898	5.13 ± 0.06
0.353 ± 0.002	0.571702	3810	17.43521	5.19 ± 0.06
0.355 ± 0.01	0.592429	60800	18.61404	5.13 ± 0.06
0.364 ± 0.02	0.599142	533000	18.07085	5.14 ± 0.07
0.392 ± 0.008	0.60186	3140000	15.36387	5.09 ± 0.05

range of solids content could be made. A suggested procedure for preparation of the dispersion requires a ratio of 71 g of polymer/g of NaOH along with 10% triethyl citrate at a final pH of ~5.[1] The ready-to-use commercial 30% dispersion Eudragit L30 D from Röhm has a pH of 2.5. At this pH, however, a 30% dispersion of the spray dried L100-55 is not stable and sediments immediately.

True polymer concentration of the latices was determined by "Loss on drying", method d (383 K, 3 h), in accordance with Ph. Eur. 1979. Taking into account the mass of compounds that did not evaporate and knowing the density of Eudragit L100-55, 1.18 g/cm^3 (data from manufacturer), the volume fraction of polymer, ϕ, was calculated.

The ζ potential of the particles was measured using a Malvern Zetasizer 4 (Malvern Instruments Ltd, Malvern, UK). Measurements were performed 24 h after preparation, on three samples from each dispersion. The latex dispersions were diluted 160-fold in an acetate buffer with similar pH and ionic strength (~10^{-2} M) prior to measurement due to their high turbidity. The used ionic strength is an estimate, since the exact degree of ionization of the carboxylic groups on the polymer is unknown.

Steady-state rheological measurements were carried out using a Bohlin VOR Rheometer (Bohlin Reologi, Lund, Sweden), a controlled strain instrument, with a double gap measuring system (DG 24/27) for dispersions of low viscosity or a concentric cylinder (C25) for dispersions of intermediate viscosity. A controlled stress instrument (Stresstech Rheometer, Reologica Instruments, Lund, Sweden) with a concentric cylinder (CC15) measuring system was used for all the dynamic viscoelastic measurements. The frequency range of 0.0001-90 Hz with a constant stress of 0.5 Pa was used. This stress is such that resulting deformation lies within the linear viscoelastic region of all dispersions measured. All measurements were performed at 298 K. Unwanted drying out and film formation at the surface of the sample were prevented by covering the measuring cups with a vapor trap. The intrinsic viscosity was determined using an Ostwald capillary viscometer at 298 K.

The glass transition temperature of the spray-dried Eudragit L100-55 was determined using modulated temperature differential scanning calorimetry (MTDSC) on a Seiko DSC220C instrument upgraded with a SSC5300 analysis system. Other operational conditions are described by Singh et al.;[13] the instrument operational parameters used were a heating rate of 3 K/min, an amplitude of 1 K, and a frequency of 0.02 Hz. The T_g of the MAEA copolymer in question here could not be detected using a conventional DSC.

To examine the effect of moisture on the glass transition temperature, samples were stored for 3−4 weeks in desiccators with constant humidity atmosphere at room temperature. The constant relative humidity atmospheres, in the range 31−95% RH, were created using saturated salt solutions.[14] Dried polymer samples were weighed (5−10 mg) into aluminum DSC pans and placed in these desiccators for equilibration. Prior to measurement, the pans were quickly sealed with crimping covers.

The water content of the MAEA powder equilibrated at the specified relative humidity was measured by Karl Fischer (coulometry) analysis (Metrohm 737 KF Coulometer, Metrohm AG, Herisau, Switzerland).

The glass transition temperature (at various moisture contents) can also be determined by an isothermal dynamic vapor sorption (DVS) method.[15] The sample is loaded onto a quartz pan of a microbalance located in a controlled gas flow environment, where the relative humidities (0−95%) can be accurately specified while the weight gain is continuously registered (DVS-1, Surface Measurement Systems, Marlow, UK). DVS was performed on the MAEA sample at one temperature (313 K) only to confirm the results of the MTDSC measurements.

Results and Discussion

The surface charge of particles in dispersions has a strong influence on both the stability and the flow behavior of the dispersion. Since the MAEA particles carry carboxylic groups, the particles will be negatively charged at the pH of the experiments (Table 1). This is confirmed by measuring the ζ potential of the particles. At $\phi = 0.25$ the ζ potential was -42 ± 1.9 mV, and at $\phi = 0.34$ the value was -43 ± 1 mV. There was a small tendency of the ζ potential to increase with increasing the polymer content. This was, however, within the uncertainty of the method. All the dispersions were therefore considered to have the same ζ potential. The ζ potential of the ready-to-use Eudragit L30D was -14 ± 3 mV in a dilution buffer of pH 2.5 and ionic strength 10^{-2} M.

In addition to the charges on the particles and the probable presence of dissolved polymer chains, the dried latex contains surface active substances that could in principle contribute to the steric stabilization of the dispersion.[16,17] Some simple experiments were performed in order to gain some insight into the interparticle repulsion/stabilization mechanism. Addition of small amounts of salt (e.g. KCl) instantaneously affected the stability causing the dispersion to flocculate irreversibly. The same effect was seen when the pH was lowered slightly. This is a typical feature of electrostatically stabilized dispersions. The freeze−thaw stability of the dispersion was good, however, which usually indicates steric stabilization.[18] Thus, a combination of electrostatic and steric stabilization is indicated for the dispersion.

From the above experiments it is also clear that the dispersion tested here cannot be described as hard spheres. The data also does not fit Einstein's law for hard spheres since the measured intrinsic viscosity, [η], is 4.7, compared to the expected hard-sphere intrinsic viscosity of 2.5. [For comparison, Raynaud et al.[19] report an intrinsic viscosity of 3.65 for a sterically stabilized dispersion of particle diameter 250 nm, while Krieger and Dougherty[20] report 3.44 for a dispersion with rigid uncharged particles with a diameter of 110 nm]. It is apparent that the effective hydrodynamic radius of the particles is increased by the adsorbed surfactants, dissolved polymer chains, and/or electroviscous effects from surface charges, forming a stabilization layer. An estimate of the effective hydrodynamic radius can be made using the expression

$$[\eta] = 2.5\left[\frac{a_H}{a}\right]^3 \quad (1)$$

where a is the core or true radius of the particles while a_H is the effective hydrodynamic radius. The (number) average particle radius of the dispersions, containing 10−40 wt % polymer is 100 nm although the particle size distribution is fairly broad ranging from 60 to 200 nm[1]. The thickness of the stabilization layer calculated from eq 1 is 23 nm.

Steady-State Shear Flow Behavior—The steady-state shear viscosity of various volume fractions of Eudragit L100-55 latex dispersions as a function of applied shear rate is plotted in Figure 1. The dispersion with lowest ϕ's showed Newtonian behavior. All dispersions above a volume fraction of $\phi = 0.4$ showed a more or less pronounced shear thinning behavior. The extent of shear thinning increased with increasing volume fraction. At very low shear rates a plateau is evident, which is an approximation of the zero shear viscosity. The experimental

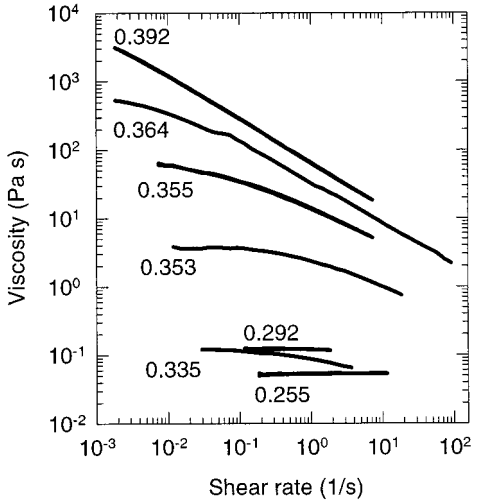

Figure 1—Steady-state shear flow curves of MAEA dispersions as a function of applied shear for increasing polymer volume fractions, ϕ ($n = 3$; see Table 1 for standard deviations). Data from controlled strain instrument.

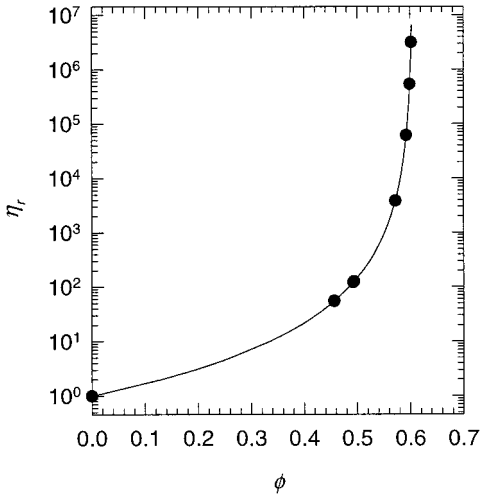

Figure 2—The low shear relative viscosity as a function of effective volume fraction for MAEA dispersions (●) fitted to the Krieger–Dougherty model, eq 3, with $[\eta] = 4.7$ and $\phi_{eff,m} = 0.605$. Data from controlled strain instrument.

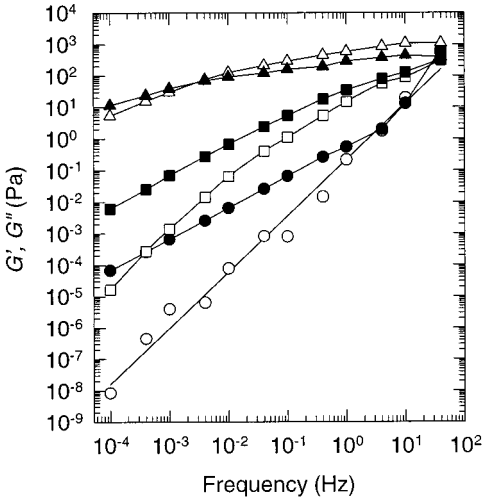

Figure 3—The storage (open symbols) and loss (closed symbols) moduli of $\phi = 0.33$ (○, ●), $\phi = 0.35$ (□, ■), and $\phi = 0.39$ (△, ▲) dispersions. Data from the controlled stress instrument.

set up could not detect the low-shear plateau for the dispersion with the highest solid content.

On the basis of previously discussed electrostatic and steric stabilization mechanism, an effective volume fraction, ϕ_{eff}, can be defined[6] such that

$$\phi_{eff} = \phi\left(1 + \frac{\Delta}{a}\right)^3 \quad (2)$$

where a is the particle radius (= 100 nm) and Δ is the increase of the effective particle radius due to contributions from the stabilization mechanisms (Debye length and/or adsorbed layer). With the above correction, the dispersion can be modeled as a hard-sphere system. The semiempirical Krieger−Dougherty equation[20] can then be used to correlate the relative viscosity, η_r, at low shear (approximation of the zero-shear viscosity from Figure 1) to the effective volume fraction

$$\eta_r = \left(1 - \frac{\phi_{eff}}{\phi_{eff,m}}\right)^{-[\eta]\phi_{eff,m}} \quad (3)$$

$[\eta]$ is the intrinsic viscosity and $\phi_{eff,m}$ is the maximum packing fraction. The value of $[\eta]$ from capillary viscometry = 4.7. The value used for $\phi_{eff,m} = 0.605$, corresponding to a hexagonally packed sphere structure (loose packing, coordination number 8). [The dispersion has a honeycomb-like structure in the last stages before the water layer disappears and the particles begin to deform and possibly coalesce.[21] Roulstone et al. propose a close-packed hexagonal structure for this stage with a maximum packing fraction of 0.74;[22] however, their conclusion is based on cast films where the particles have a longer time to achieve such a structure. Heterodispersity can also lower the packing efficiency[10]]. The value of Δ used to fit the experimental data points in Figure 2 to eq 3 are tabulated in Table 1, in accordance with Prestidge and Tadros.[23] At the low volume fractions, the effective thickness of the stabilization layer, Δ, is estimated to be 21 nm. The thickness of this stabilization layer decreases gradually with increasing volume fraction (Table 1). This is not surprising since the layer is compressed with increasing volume fractions as the particles approach each other closely. This compression causes the dispersion to display an increasingly elastic behavior as discussed below.

Viscoelastic Behavior—The viscoelastic response of the MAEA dispersion, in terms of the storage (G') and loss (G'') moduli, is shown in Figure 3 for three volume fractions. For $\phi = 0.33$ ($\phi_{eff} = 0.49$) which corresponds to a less-than-close packing fraction, G'' is considerably larger than G' at low frequencies. When the frequency is increased, the difference between the moduli decreases and at a critical value called the crossover frequency ~1 Hz, they are equal.

Increase in G' with frequency is a function of the relaxation time scale, τ_r, of the suspension in relation to the experimental time scale. At low frequencies, the experimental time of the order of $\tau \approx 1/\omega$ is longer than the relaxation time allowing the perturbed structure to relax during oscillation. The applied energy is thus dissipated, resulting in a large loss modulus or viscous behavior. With increasing frequency, τ becomes of the order of τ_r, resulting in a combined viscous and elastic response. Further increases in frequency will thus result in a predominantly elastic response i.e.,

$$G^* \approx G' = G_\infty$$

implying that the viscoelastic properties do not change at higher frequencies.[24]

With increasing volume fraction the average distance between the particles decreases causing increasing overlap of the stabilization layers surrounding the particles and

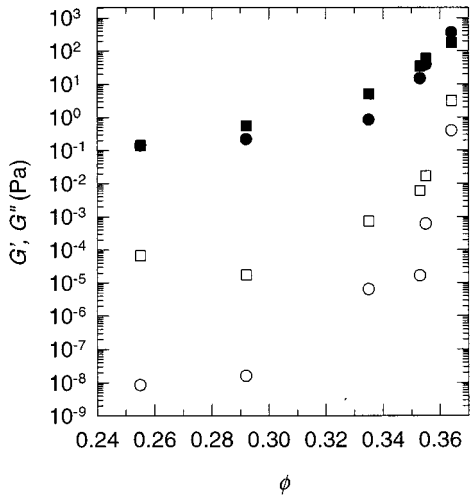

Figure 4—The storage (○, ●) and loss (□, ■) moduli at 10^{-4} Hz (open symbols) and 1 Hz (closed symbols) as a function of increasing volume fraction. Data from the controlled stress instrument.

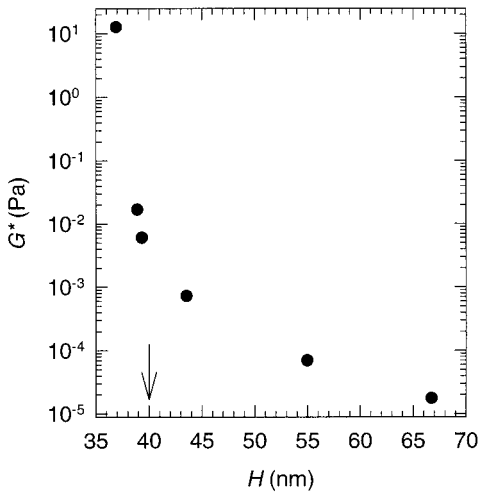

Figure 5—Complex modulus (at 10^{-4} Hz) as a function of the mean interparticle spacing from eq 5. The arrow shows the estimated point where the particles start overlapping. Data from the controlled stress instrument.

therefore increasing the elasticity (G'). This is apparent in Figure 3 for $\phi = 0.39$ ($\phi_{eff} = 0.60$). G' and G'' of this dispersion is almost frequency independent. A much lower crossover frequency is obtained, ≈0.002 Hz, since the dispersion is unable to scatter the applied energy due to its high solid content and begins to show elastic behavior at low levels of perturbation.

At low volume fractions ($\phi = 0.33$) the dispersion follows the Maxwell model, implying that one relaxation process dominates the dynamic properties of the latex in solution. The implication is that transient structures (stabilization layer) existing in the system at these concentrations are similar. [The slope of $G'(\omega)$ in Figure 3 is 1.8, and the slope of $G''(\omega)$ is 1.1, compared to 2 and 1, respectively, as required by the model]. The dispersions with higher volume fractions, however, do not fit the Maxwell model: for $\phi = 0.39$ ($\phi_{eff} = 0.60$), the slope for $G'(\omega)$ is 0.4 and for $G''(\omega)$ is 0.27 in Figure 3. This is not surprising since stabilization layer overlap and the resulting interactions introduce a new type of "cross-link" in the dispersion.

The variation of G' and G'' with volume fraction at two different frequencies of oscillation are shown in Figure 4, where an increase in solid content increases G'' and particularly G'. The phase angle shift is almost 90° for the lowest volume fractions but increases to approximately 45°, at $\phi = 0.36$ ($\phi_{eff} = 0.60$). Results from both frequencies confirm that the close-packing volume fraction for the present system occurs at $\phi_{eff} = 0.60$, above which the system behaves as a gel.[23]

The reciprocal crossover frequency (in rad/s) can be used to approximate the relaxation time, assuming that the material follows the Maxwell model of viscoelastic fluids. The relaxation time increases with the volume fraction and typical values of the relaxation time are 0.1 s for the low ($\phi_{eff} = 0.49$) concentration increasing to ~75 s for the high solid dispersions ($\phi_{eff} = 0.60$). To put these in perspective, characteristic process times for spraying are of the order of 10-5 s, while that for leveling of an applied film is 100 s. These times thus agree well with the characteristic relaxation times of the dispersions at the relevant concentrations. To further relate the viscoelastic properties to the deformation and possible coalescence processes, we resort to the modified viscoelastic model[9] for film formation by Eckersley and Rudin.[2] According to this model, film formation requires

$$G'(t) \leq \frac{34\sigma}{a} \tag{4}$$

where σ is the surface tension of water in the capillaries between particles, while $G'(t)$ is the time-dependent elastic shear modulus of the polymer. Using $\sigma = 30$ mN/m and 200 nm as the largest particle size in the dispersion gives a critical upper limit for elastic modulus of 5.1×10^6 Pa. Figure 4 shows that this criteria is satisfied by the present dispersion.

The mean interparticle spacing in a dispersion, H, is a measure of the closeness of approach of these particles and can be expressed as

$$H = 2a\left[\left(\frac{\phi_{eff,m}}{\phi_{eff}}\right)\right] \tag{5}$$

In Figure 5, we have plotted the complex modulus G^* (at 1 Hz) against H calculated from eq 5 using values of ϕ from Table 1 and $\phi_m = 0.605$ as indicated above. It is clearly apparent that as the interparticle spacing falls below 40 nm, G^* increases markedly due to the stabilization layers beginning to overlap. An estimate of the thickness of this layer is therefore $= {}^1/_2H$, i.e., approximately 20 nm. This value compares well to the Δ-value in Table 1 for the low volume fractions, as well as the estimate from intrinsic viscosity using eq 1.

The Debye double layer thickness, $1/\kappa$, in the present system (water at 298 K)

$$\kappa = 3.288\sqrt{I} \quad (\text{in nm}^{-1}) \tag{6}$$

gives a fairly thin double layer of the order of 3 nm, due to the ionic strength estimated as 10^{-2} M. The large value of κ_a (≈ 30) suggests that primary electroviscous effects would be small. Secondary electroviscous effects, while not significant at low volume fractions, may, however, play a role in increasing the viscosity at the high volume fractions considered here. In the literature, such effects have been attributed to the formation of (temporary) doublets of like-charged particles which allow energy to be dissipated when rotating in or when destroyed by shear.[25] Examining the possible steric contributions to the stabilization layer suggests that the surfactants added to the latex particles (Polysorbate 80 and SLS) cannot extend out 20 nm from the surface of the particles. This and the fairly high ζ potential imply that alternative explanations are needed to rationalize the extent of the stabilization layer (which is in agreement when calculated from the various methods). This layer must arise due to dissolved latex polymer chains

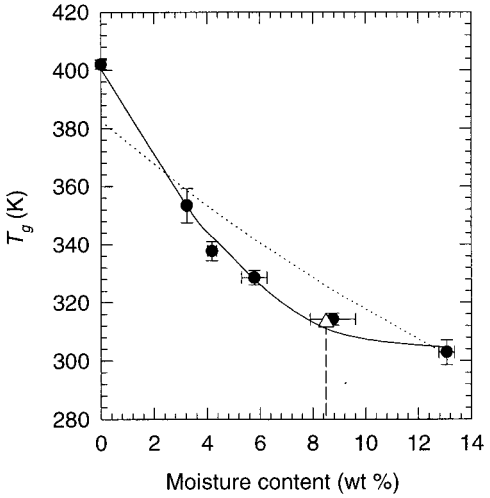

Figure 6—Influence of moisture content on T_g for spray-dried MAEA dispersion from MTDSC (●). The dotted line is calculated from eq 7 while the continuous line is a data fit using eq 9. Standard deviations are shown for both T_g and the moisture content. Results of T_g determination by DVS (Δ) at 40 °C (313 K) is marked with a line.

Table 2—Moisture Sorption Isotherm at 25 °C, and the Glass Transition Temperature (T_g) of Eudragit L 100-55 (Methacrylic Acid–Ethyl Acrylate Copolymer) ($n = 3$)

rel humidity (%)	equilibrium moisture content by KF (wt %)	equilibrium moisture content by DVS (wt %)	T_g by MTDSC (K)
0	0	0	402 ± 1.6
31	3.24 ± 0.05	3.68	353 ± 5.8
42	4.19 ± 0.17	4.70	338 ± 3.3
58	5.78 ± 0.48	6.70	329 ± 2.5
90	8.76 ± 0.86	10.9	314 ± 2.0
95	13.1 ± 0.29	13.8	303 ± 4.2

which allow the charged carboxyl groups to extend further out from the surface. The alkyl chain of anionic SLS can also adsorb to the surface of the latex as well as bind to the dissolved chains extending the charged headgroup into the surrounding phase, effectively increasing the (negative) surface charge. The picture we have of the latex is thus one with a charged "hairy" surface, electrosterically stabilized.[26] The presence of the adsorbed neutral surfactant (as well as dissolved polymer) can influence the adsorption characteristics of the ions in the diffuse layer as well as shifting the shear plane away from the surface. Contribution to the latter effect due to Polysorbate 80 will not be very strong since the amount added is small, allowing the adsorbed layer to be approximated as free draining; any contribution due to dissolved latex polymer is, however, difficult to estimate. Change in the ion distribution in the diffuse layer can be caused by excluded volume effect leading to an extension of the double layer and thereby an increase in the surface potential of the particle.[25]

Moisture Sorption and Thermal Analysis—MAEA is an amorphous polymer and takes up water in a humid environment. The moisture sorption isotherm at 298 K is tabulated in Table 2 and shows good agreement between the two (KF and DVS) techniques. The particles absorb up to 13% moisture when exposed to high relative humidity. The data seems to follow a typical Type II isotherm for multilayer physical adsorption on nonporous solids.

The corresponding T_g of the MAEA particles (measured by MTDSC) equilibrated at a range of relative humidities is also shown in Table 2 and plotted in Figure 6. The glass transition temperature of the particles is substantially lowered after exposure to moisture, as is to be expected. Lehmann[1] reports the MFT of redispersed MAEA latex is 291 K, the MFT of the ready-to-use Eudragit L30D dispersion is 300 K, and the T_g of the dry polymer is 380 K. We find that the T_g (at high moisture content; Figure 6) is a good first approximation of the MFT. The data also suggests that since the T_g (and thus MFT) rises rapidly with decreasing water content, the process of film formation should be complete before the sprayed material is dried to such an extent that the MFT rises above operating temperature. A balance is therefore required between spray rate, temperature, and drying air flow. It also implies that the MFT of (and T_g for hydrophilic) latex systems must be related to the moisture content, and determined by the humidity of the drying air in which it is measured.

The data from the Dynamic Vapor Sorption measurement performed at 313 K agrees well with the MTDSC data as shown in Figure 6. A glass transition event at this temperature is detected when the moisture content of the polymer is approximately 9%. However, no such event is observed when the experiment is performed at 298 K. The plasticizing effect of sorbed moisture is not sufficient to lower the T_g to 298 K.

Monotonic variations of the T_g with composition in mixtures/blends are often modeled by the modified Gordon−Taylor equation which is based on free volume effects under the assumption that there are no specific interactions between the components. For a three-component mixture, this can be written as

$$T_{gmix} = \frac{w_1 T_{g1} + K_{12} w_2 T_{g2} + K_{13} w_3 T_{g3}}{w_1 + K_{12} w_2 + K_{13} w_3} \quad (7)$$

where w_1, w_2, and w_3 are the weight fractions of the three components, and T_{g1}, T_{g2}, and T_{g3} are the corresponding pure component glass transition temperatures. Constants K_{12} and K_{13} are ratios of free volumes of components and can be estimated from

$$K_{ij} = \frac{\rho_i T_{gi}}{\rho_j T_{gj}} \quad (8)$$

where ρ_i represents density of component i.

We expect that the MAEA copolymer has specific interactions with water including deprotonation of the carboxylic groups. Similarly, hydrophobic portions of Polysorbate 80 will have an increased affinity for the latex surface. To account for these interactions, quadratic and third-power interaction terms are added to eq 7, giving

$$T_{gmix} = \frac{w_1 T_{g1} + K_{12} w_2 T_{g2} + K_{13} w_3 T_{g3}}{w_1 + K_{12} w_2 + K_{13} w_3} + Q_{12} w_1 w_2 + Q_{13} w_1 w_3 + Q_{123} w_1 w_2 w_3 \quad (9)$$

where Q_{12}, Q_{13}, and Q_{123} are empirical interaction parameters reflecting the strength and type of interactions.[27,28] We denote MAEA, water and Polysorbate 80 as components 1, 2, 3 with T_{g1}, T_{g2}, and T_{g3} as the glass transitions temperatures of pure MAEA, water (= 135 K),[29] and Polysorbate 80 (= 207 K), respectively. The T_g of Polysorbate 80 was measured in this work, but the same could not be done for pure MAEA since the MAEA available was preblended with surfactants. While an extensive dialysis procedure could in principle remove all added surfactant, we chose to estimate this parameter (T_{g1}) from the data at 0% RH. We have neglected any plasticizing effect of SLS because of the small amount added. Using a two-component version of eq 7 on T_g data at 0% RH gives T_{g1} = 412 K. (Specific gravity of Polysorbate 80 = 1.08 and of MAEA = 1.18). Utilizing this parameter in eq 7 to calculate the T_{gmix}

of the blend at various moisture contents gives a theoretical glass transition that does not agree with the experimental data (Figure 6). However, using eq 9 with Q_{12} and Q_{123} as curve-fitting parameters allows the data to be modeled well as shown in Figure 6. (It was found that the parameter Q_{13} could be dropped without any effect on the goodness of fit). The value obtained for parameter Q_{12} is positive while that for Q_{123} is negative. While Kwei et al. have presented arguments based on intermolecular force parameters to explain the negative values of such parameters,[30] we will simply ascribe these to be empirical parameters that enable the data to be modeled and underline the importance of specific interaction terms in our system.

Conclusions

In the first part of this study, we have used the techniques and methods of colloid science and applied them to a technical latex, widely used in the pharmaceutical industry. The dispersions are found to be electrostatically and sterically stabilized. The stabilization is considered to arise in part from dissolved polymer chains with charged groups that extend out into the bulk continuous phase. The extent of the stabilization layer was estimated to be around 20 nm, giving an effective hard-sphere volume that can be used to relate the steady shear and viscoelastic properties to the film formation phenomena. The presence of dissolved polymer chains in the dispersion implies that coalescence and interpenetration will be facilitated during film formation.

The results generated here provide a baseline to evaluate the effect of normal coating additives such as plasticizers, colorants, flavorants, buffering agents etc., on dispersion stability and film-forming ability. While such studies increase our understanding of the systems in question, they also point to the complexity and limitations in the strict application of techniques and models based on ideal and simplified systems. Technical dispersions present a challenge because of their heterodispersity and the combination of mechanisms involved.

The glass transition temperature of the particles making up the dispersion has then been determined as a function of sorbed moisture and modeled by the Gordon−Taylor equation modified for specific interaction between water, surfactant, and polymer. Our data and that in the literature suggests that the high-moisture content T_g can be used as a first approximation for the MFT. Change in T_g (and thus MFT) with moisture content implies that the process must be controlled so as to produce a rate of drying slow enough to allow coalescence to occur. A curing stage is generally added to assist in the coalescence and interpenetration of the sprayed polymer chains. Knowledge of the moisture sorption and T_g data can be used to determine the conditions of this stage especially for heat labile substances.

References and Notes

1. Lehmann, K. Chemistry and application properties of polymethacrylate coating systems. In *Aqueous Polymeric Coatings for Pharmaceutical Dosage Forms*, 2nd ed.; McGinity, J. W., Ed.; Marcel Dekker: New York, 1997; pp 101−176.
2. Eckersley, S. T.; Rudin, A. Mechanism of Film Formation from Polymer Latexes. *J. Coat. Technol.* **1990**, *62*, 89−100.
3. Lin, F.; Meier, D. J. A study of latex film formation by atomic force microscopy. 1. A comparison of wet and dry conditions. *Langmuir* **1995**, *11*, 2726−2733.
4. Lin, F.; Meier, D. J. A study of latex film formation by atomic force microscopy. 2. Film formation vs rheological properties: Theory and experiment. *Langmuir* **1996**, *12*, 2774−2780.
5. Dobler, F.; Hall, Y. Mechanism of latex film formation. *Trends Polym. Sci.* **1996**, *5*, 145−151.
6. Tadros, T. F. Use of viscoelastic measurements in studying interactions in concentrated dispersions. *Langmuir* **1990**, *6*, 28−35.
7. Wang, Y.; Juhué, D.; Winnik, M. A.; Leung, O. M.; Goh, M. C. Atomic force microscopy study of latex film formation. *Langmuir* **1992**, *8*, 760−762.
8. Heuts, M. P. J.; le Fêbre, R. A.; van Hilst, J. L. M.; Overbeek, G. C. Influence of morphology on film formation of acrylic dispersions. *Film formation in waterborne coatings*; Provder, T., Ed.; ACS Symposium Series, 648, American Chemical Society: Washington, DC, 1996; pp 271−285.
9. Brown, G. L. Formation of films from polymer dispersions. *J. Polym. Sci.* **1956**, *22*, 423−434.
10. Keddie, J. L.; Meredith, P.; Jones, R. A. L.; Donald, A. M. Kinetics of film formation in acrylic latices studied with multiple-angle-of-incidence ellipsometry and environmental SEM. *Macromolecules* **1995**, *28*, 2673−2682.
11. Lippold, B. C.; Lippold, B. H.; Sutter, B. K.; Gunder, W. Properties of aqueous, plasticizer-containing ethyl cellulose dispersions and prepared films in respect to the production of oral extended release formulations. *Drug Dev. Ind. Pharm.* **1990**, *16*, 1725−1747.
12. Hoy, K. L. Estimating the effectiveness of latex coalescing aids. *J. Paint. Technol.* **1973**, *45*, 51−56.
13. Singh, S. K.; Jalali, A. F.; Aldén, M. Modulated temperature differential scanning calorimetry for examination of tristearin polymorphism. I. Effect of operational parameters. *J. Am. Oil Chem. Soc.*, in press.
14. Nyqvist, H. Saturated salt solutions for maintaining specified relative humidities. *Int. J. Pharm. Technol. Prod. Manuf.* **1983**, *4*, 47−48.
15. Buckton, G.; Darcy, P. Water mobility in amorphous lactose below and close to the glass transition temperature. *Int. J. Pharm.* **1996**, *136*, 141−146.
16. Florence, A. T.; Rogers, J. A. Emulsion stabilization by nonionic surfactants: experiment and theory. *J. Pharm. Pharmacol.* **1971**, *23*, 153−169.
17. Zapata, M. I.; Feldkamp, J. R..; White, J. L.; Hem, S. L. Use of the tension cell to monitor particle interactions in suspensions. *Drug Dev. Ind. Pharm.* **1989**, *15*, 1933−1941.
18. Zapata, M. I.; Feldkamp, J. R..; Peck, G. E.; White, J. L.; Hem, S. L. Mechanism of freeze−thaw instability of aluminum hydroxycarbonate and magnesium hydroxide gels. *J. Pharm. Sci.* **1984**, *73*, 3−8.
19. Raynaud, L.; Ernst, B.; Vergé, C.; Mewis, J. Rheology of aqueous latices with adsorbed stabilizer layers. *J. Colloid Interface Sci.* **1996**, *181*, 11−19.
20. Krieger, I. M.; Dougherty, T. J. A mechanism for nonnewtonian flow in suspensions of rigid spheres. *Trans. Soc. Rheol.* **1959**, *3*, 137−152.
21. Barnes, H. A.; Hutton, J. F.; Walters, K. Rheology of suspensions. In *An Introduction to Rheology;* Elsevier B. V.: Amsterdam, 1989; pp 115−139.
22. Roulstone, B. J.; Wilkinson, M. C.; Hearn, J.; Wilson, A. J. Studies on polymer latex films: I. A study of latex film morphology. *Polym. Int.* **1991**, *24*, 87−94.
23. Prestidge, C.; Tadros, T. F. Viscoelastic properties of aqueous concentrated polystyrene latex dispersions containing grafted poly(ethylene oxide) chains. *J. Colloid Interface Sci.* **1988**, *2*, 660−665.
24. Bergström, L. Rheology of concentrated suspensions. In *Surface and Colloid Chemistry in Advanced Ceramics Processing;* Pugh, R. J., Bergström, L., Eds.; Marcel Dekker Inc.: New York, 1994; pp 193−244.
25. Hunter, R. J. Charge and potential distribution at interfaces. In *Zeta Potential in Colloid Science, Principles and Applications*; Academic Press: London, 1981; Ch. 2, 5, 8.
26. Peula, J. M.; Santos, R.; Forcada, J.; Hidalgo-Alvarez, R.; de Las Nieves, F. J. Study on the colloidal stability mechanisms of acetal-functionalized latexes. *Langmuir* **1998**, *14*, 6377−6384.
27. Kwei, T. K. The effect of hydrogen bonding on the glass transition temperatures of polymer mixtures. *J. Polym. Sci., Polym. Lett. Ed.* **1984**, *22*, 307−313.
28. Hancock, B. C.; Zografi, G. The relationship between the glass transition temperature and the water content of amorphous pharmaceutical solids. *Pharm. Res.* **1994**, *11*, 471−477.
29. Sugisaki, M.; Suga, H.; Seki, S. Calorimetric study of the glassy state. 4. Heat capacities of glassy water and cubic ice. *Bull. Chem. Soc. Jpn.* **1968**, *41*, 2591−2599.
30. Kwei, T. K.; Pearce, E. M.; Pennacchia, J. R.; Charton, M. Correlation between the glass transition temperatures of polymer mixtures and intermolecular force parameters. *Macromolecules* **1987**, *20*, 1174−1176.

JS9803555